Journal of Membrane Science & Research

journal homepage: www.msrjournal.com

Research Paper

Synthesis of Polyvinyl Chloride-Based Zirconium Molybdophosphate Composite Membrane: An Assessment of Experimental and Theoretical Approaches through Electrochemical Parameters

Aiman Zehra [1], Mohd Arsalan [2], Rafiuddin [1,*]

[1] *Department of Chemistry, Aligarh Muslim University, Aligarh-India*
[2] *Department of Applied Chemistry, Aligarh Muslim University Aligarh-India*

Article info

Received2022-05-11
Revised 2023-01-17
Accepted2023-01-17
Available online2023-01-17

Keywords

Polyvinyl chloride-based zirconium Molybdophosphate
Theoretical applicability
Structural characterization
Electrochemical observation
Separation process

Highlights

- Polyvinyl chloride-based zirconium molybdophosphate composite membrane
- Selection of the appropriate ratio of polymer and filler for the highest stability and selectivity
- Composite membrane has the combination of PVC and ZMP in a 25% and 75% ratio, respectively
- The membrane was characterized by SEM, TEM FTIR, TGA, and EDX analysis
- The electrochemical properties have been studied to render the applicability in different separation processes

Graphical abstract

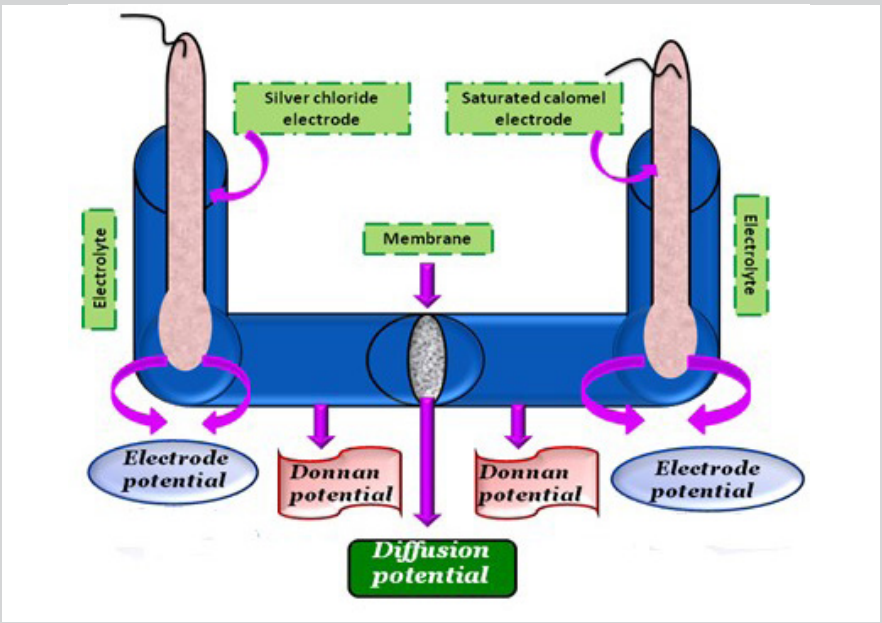

Abstract

The Polyvinyl chloride (PVC) based zirconium molybdophosphate (ZMP) composite membrane was designed through the important die-casting process. The preparation of this cation exchange membrane is being used to enhance the stability and electrochemical properties. The selection of an appropriate ratio of polymer and filler for attaining the membrane of the highest stability and selectivity has been done by comparing various ratios in terms of ion exchange capacity, water uptake, porosity, membrane potential, and chemical and thermal stability. The used inorganic material was synthesized by the sol-gel method of material synthesis, and the synthesized composite membrane has a combination of PVC polymer and ZMP inorganic material in a 25% and 75% ratio, respectively. The membrane was characterized by using various techniques including SEM, TEM, FTIR, TGA, and EDX analysis, which verified the functional groups, material nature, thermal stability, surface structure, porosity, elemental percentage, ion transportation, etc. The synthesized membrane has indicated appropriate ion-exchange capacity, high stability, reproducibility, and selectivity for salts and heavy metal ions. The electrochemical properties have been studied to determine their applicability in different separation processes.

1. Introduction

Water exists in many forms, such as a liquid or a solid, as in snow and ice; underneath the land surface as groundwater; and in the atmosphere, as in clouds and invisible water vapor. About 70% of the surface of our planet, earth, is covered in water. We are nestled in our solar system at just the right distance from the sun for this liquid water to exist. Water cannot exist naturally as H_2O alone. The reason for this is that water is a universal solvent, and it easily dissolves a variety of materials [1]. Some of these materials, such as naturally occurring minerals, are good additions, while others shouldn't be

* Corresponding author: rafi_amu@rediffmail.com (Rafuddin)

DOI: 10.22079/JMSR.2023.553575.1545

advantageous for human life. The types of impurities in the water can include dust, dirt, harmful chemicals, biological contaminants, radiological contaminants, and total suspended solids (TSS). Total suspended solids are visible particles that can make water appear cloudy or hazy [2]. Water from rainfall, streams, and wells can pick up harmful chemicals in the environment like acid and metallic elements. Biological components in water can include bacteria, algae, organic waste, amino acids, pathogens, viruses, microbes, and parasites [3]. They end up in the water because of contact with industrial sewage and wastewater, agricultural waste and runoff, decomposing waste in water bodies, and imbalances in water chemical profiles that promote the proliferation of microbes. To remove general impurities such as floating and suspended matter, colloidal particles, dissolved organic matter, and the destruction of disease-causing microorganisms, common water treatment processes such as flocculation, sedimentation, filtration, and disinfection are used [4].

Ion exchange is a water treatment process commonly used for water softening or demineralization, but it is also used to remove other substances from the water in processes such as dealkalization, deionization, denitrification, and disinfection [5]. In other words, ion exchange is a water treatment method where one or more undesirable ionic contaminants are removed from water by exchange with another non-objectionable or less objectionable ionic substance [6]. A membrane can be defined as an interface between two adjacent phases, functioning as a selective barrier and regulating the transportation between them. Symmetric membranes have uniform pore size or structural morphology throughout the cross-section of the membrane and are widely used in dialysis processes, while asymmetric membranes are anisotropic structures comprising two main layers with diverse properties, such as morphology and permeability. Asymmetric membranes are typically distinguished by a relatively dense and extremely thin top layer that is supported by an open, much thicker porous substructure indicated by the bottom layer [7, 8].

These types of membrane systems are used in many filtration as well as separation processes. The composite or anisotropic structures of membranes show the processes of desalting under some pressure gradients, which are indicated particularly by nanofiltration and reverse osmosis membrane due to their high salt rejection, volume flux, and mechanical stabilities. The composite membranes are commonly used in advanced molecular separation processes i.e. reverse osmosis, nanofiltration, pervaporation, and membrane adsorption [9]. Now these days membrane technology-based chemical separation processes comprise an emerging field of research and industrial technology. The main objective of this research is to develop membranes that selectively transport particular targeted molecules/ions having definite sizes or shapes, and discarded (or transport at much lower rates) the other types of molecules/ions that might be present in the feed solution or gases environment. The important property of such cation and anion-exchange membranes is to selectively permeate the particular ions through the synthesized composite membrane. Being potentially less energy-intensive than other competing separation methods is a key feature of membrane-based technologies, and as such, they can be seen as an example of "green chemistry." However, geometries that call for a high flux of the desired target molecule can contain materials with superior chemical selectivity. [10, 11]. Because of variations in their concentrations, the membrane's pore diameters, and interactions with the electrolyte, ions transform when they pass through a charged membrane [12].

A charged membrane can also segregate electrolyte ions based on the charge of the membrane. Recently, it has become necessary to analyze the ion transport phenomena specifically in aqueous, organic, and electrolyte solution systems across a charged membrane from the point of industrial and medical applications. The pore size distribution is the primary factor that determines how well a composite membrane separates particles [13]. Particles that are larger than the membrane's pore size are rejected, while smaller particles can easily pass across the membrane barrier. As a result, the membrane pore size distribution is the only factor used to determine membrane filtration [14]. The thickness of the membrane is inversely proportional to the rate at which transferable particles permeate it because the barrier to mass transfer in these types of membranes is determined by their thickness and porosity. [15].

The fabrication of ion-exchange inorganic-organic composite membranes can be done by using coating techniques to produce highly selective thin and dense membranes with relatively high flux [16]. While the ion-exchange inorganic-organic composite materials can be synthesized by several processes like sol-gel, co-precipitation, intercalation, blending, in situ polymerization, molecular self-assembling, etc., the sol-gel process is one of the most common and qualitative methods of material synthesis. Many researchers used the sol-gel or liquid coupling processes of silane coupling agents to prepare a hybrid anion exchange membrane [17–18]. This work focuses on the synthesis, characterization, and electrochemical studies of PVC-based ZMP composite membranes. Various characterization techniques were used for examining the structural, thermal, and chemical stabilities using FTIR, TG/DTA, SEM, and XRD. Membrane potential, fixed charge density, mobility ratio, and transport numbers have been calculated using the TMS equation and experimental results were compared to theoretical results [19].

2. Materials and methods

2.1. Reagents and chemicals

Zirconylchloride (Otto Kemi, 99%), Sodium molybdate (Merck, 99%, Mumbai, India), Ortho phosphoric acid (Fischer Scientific), and polyvinyl chloride (Otto Kemi, Mumbai, India) were used for fabrication of the membrane. Various electrolyte solutions, including NaCl and $NaNO_3$ (Merck, India), KCl (Otto Kemi), and KNO_3 (RFCL, New Delhi, India) were also prepared for later experiments [20].

2.2. Fabrication of PVC/ ZMP composite membrane

Organic–inorganic composite membrane material has been prepared by the sol-gel technique. Aqueous solutions of 0.1 M sodium molybdate and 0.1 M zirconyl chloride prepared in double distilled water were mixed and stirred well using a mechanical agitator for thorough mixing. To this mixture, 0.1M orthophosphoricacid (Fischer scientific) was added with constant stirring to obtain zirconium molybdophosphate gel, and the pH of the mixture was maintained to neutral by adding HCl/NaOH, which was then left for ageing at room temperature for 24 h. The supernatant liquid was decanted off and the precipitate was washed with distilled water to get a pure gel, which was then collected and dried for 2 hours in an oven [21, 22]. The solid thus formed was grounded to a fine powder and sieved to get a particular size of 200 meshes using a sieve of the same size. On the other hand, PVC sieved with the same mesh size was mixed with ZMP to form a composite material. The appropriate mixing ratio is significant during fabrication. Studies showed that 25% polymer and 75% inorganic material come out to be the most stable ratio. Other than this, other than this results in instability of the membrane. Mixing was carried out using a mortar and pestle for 2 hours to make a homogeneous mixture. The composite material thus formed was then heated and placed in a pressure device (hydraulic press, SL 89, UK) applying a pressure of 70 MPa and the membrane was formed [23].

2.3. Physicochemical characterization

A (MiniFlex Benchtop) X-ray Diffractometer was used to record the X-Ray Diffraction (XRD) pattern for the analysis of the crystallographic structure of the synthesized membrane. FTIR spectral studies (Interspec 2020 FT-IR spectrometer, Spectrolab UK) have been performed for the elucidation of functional groups present on the membrane. Studies for thermal analysis of the membrane material were carried out using thermo gravimetric analysis (TG/DTA) by Shimadzu DTG-60 H, using a nitrogen atmosphere with a speed of 20o/min. To reveal the surface morphology and chemical composition of the synthesized membrane, Scanning Electron Microscopy (SEM) and EDS studies using JEOL JSM 651O LV were also carried out. Determination of all those parameters that affect the membrane stability and electrochemical properties is an important requirement for understanding the performance of the membrane [24]. These parameters include water content, volume void porosity, ion exchange capacity, swelling, and chemical stability determination of the membrane and are described below [25].

2.3.1. Water percentage, volume void porosity

Water percentage, volume void porosity, and swelling were measured by dipping the membrane in distilled water for 10 hours and soaking the moisture with filter paper. Then the wet membrane, with no water molecules left on the surface, was weighed. The membrane was then dried at 100 ºC and weighed again. Putting the wet and dry weight of the membrane in formulae for each parameter (discussed in the result and discussions section), the values were calculated [26]. The water percentage of the membrane is calculated by the following equation 1:

$$Water\ percentage = \left(\frac{W_{wet} - W_{dry}}{W_{dry}}\right) \times 100 \quad (1)$$

where, W_{dry} is the weight of the dry membrane and W_{wet} is the weight of the membrane after it has been dry for four to five hours of soaking in water. Equation 2 has been used to compute the membrane's volume void porosity in (g/cm^2).

$$Volumetric\ porosity\ (\%) = \left(\frac{Ww - Wd}{AL\rho w}\right) \times 100 \quad (2)$$

where A is the area of membrane, L is themembrane thickness, and $\rho_w$is density of water.

2.3.2. Diameter, thickness, and swelling of the membrane

The diameter, thickness, and swelling of the membrane are easily replicated by the screw gauze equipment, which has an average thickness of 4-5ths. The difference between the average thickness that is equilibrated in 1 M NaCl solution and the dry membrane can also be used to quantify swelling. Table 1 shows the thickness, porosity, swelling, and diameter of PVC/ZMP composite membranes.

Table1
Thickness, porosity, swelling, and diameter of PVC/ZMP composite membranes.

Applied Pressure (MPa)	Diameter (cm)	Thickness (µm)	Water content (%)	Porosity (g/cm^2)	Swelling
100	2.45	60	0.030	0.020	No swelling

2.3.3. Ion exchange capacity

The acid-base titration method was employed for the determination of IEC. The membrane was soaked in 0.1 M NaCl solution and left overnight, ensuring the complete exchange of captions (H^+ with Na^+). An IEC value was obtained by titrating the solution containing all the substituted protons with a 0.01 M NaOH solution using phenolphthalein as an indicator. The total number of H+ was obtained and calculated using the following formula [27].

$$IEC\ (meq\ g^{-1}) = \frac{N \times V}{W} \quad (3)$$

where N and V are representing the normality and volume of the NaOH solution respectively and W is the mass of the membrane in grams. The membrane was regenerated by placing it in 0.1 M HCl solution to convert it into H^+ form for future use.

2.3.4. Chemical stability

The chemical stability of the membrane was examined in alkaline, acidic, neutral, and oxidant media. Freshly prepared membranes were dipped in increasing strengths of harsh acids such as H_2SO_4 and HNO_3, alkalis such as NaOH, and in oxidant media such as $K_2Cr_2O_7$ and $KMNO_3$ up to 1M at room temperature for 24 hours [28].

2.3.5. Membrane potential measurements

The membrane potential of the PVC/ZMP membrane was determined by a digital potentiometer as described in previous work. 1M TO 0.001 M concentrations of four different electrolytes, including $NaNO_3$, KNO_3, NaCl, and KCl, were taken as electrolytes into the 5 series. Following, Fig. 1 shows the electrochemical setup for membrane potential determination.

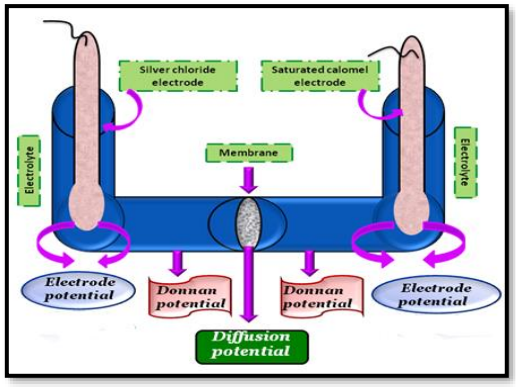

Fig. 1. Electrochemical setup used for membrane potential determination.

3. Results and discussions

The FTIR spectra of pure inorganic material and that of a composite are demonstrated in Fig. 2. The peaks at 3415 cm^{-1}, 1182 cm$^{-1,}$ and 1626 cm^{-1} correspond to the strongly bonded water molecules and the characteristic stretching vibrations of phosphate and molybdate groups, respectively. While the PVC-based inorganic material shows various peaks at different ranges. The peak around 3500 cm^{-1} indicated the presence of water molecules. The peak at higher wavenumber shows the asymmetric stretching bond of C−H and the lower peak is for the symmetrical stretching bond of C−H. The peak around 1250 cm^{-1} is attributed to the bending bond of C−H near Cl. The C−C stretching bond of the PVC backbone chain occurs in the range of 1000−1100 cm^{-1}. Finally, peaks in the range of 600−650 cm^{-1} correspond to the C−Cl gauche bond present in the composite material.

These peaks, along with the intensity change of the bands, clearly represent the composite formation. The lack of clear peaks in the XRD spectra of Fig. 3 indicates that the composite material is semi-amorphous. However, broad peaks at 2θ = 100, 270, and 470 show the presence of PVC, zirconium phosphate, and molybdate groups respectively [29].

TG/DTA was utilized to examine the thermal strength of the composite material presented in Fig. 4. The DTA curve represents one endothermic peak at 117 ^{0}C, showing the removal of atmospheric moisture. Two degradation stages have been shown by the TGA curve. The first stage occurs between 70 ^{0}C and 175 ^{0}C and corresponds to minimizing absorbed moisture with an 8.6% weight loss, whereas the second stage represents PVC thermal oxidation and occurs between 310 ^{0}C and 400 ^{0}C. SEM micrograph Fig.5 of the composite material represents the homogenous nature of the membrane with pores distributed all over the surface uniformly, and it shows no visible cracks and aggregations. EDX analysis shown in Fig. 6 confirms the composition of the uniform composite formation indicates the various percentages of elements in the material. EDX is an analytical method for the analytical or chemical characterization of materials. EDX systems are generally attached to an electron microscopy instrument. It indicated a quick, non-destructive determination of the elemental composition of the sample [30].

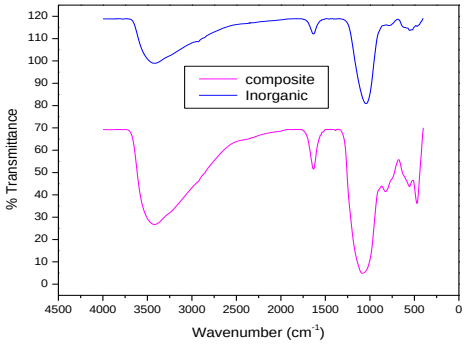

Fig. 2. FTIR spectra of ZMP and PVC/ZMP composite materials.

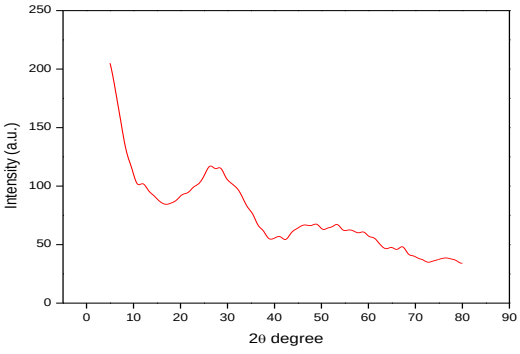

Fig. 3. XRD spectrum of PVC/ZMP composite material.

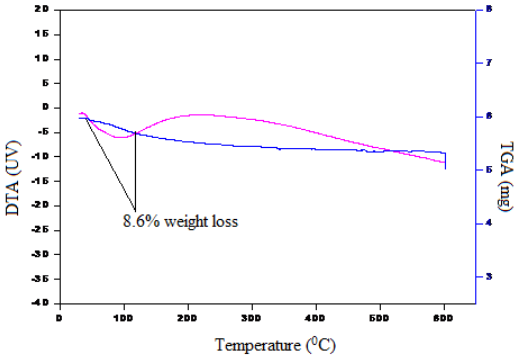

Fig. 4. TG/DTA curves for the thermal stability determination of PVC/ZMP composite.

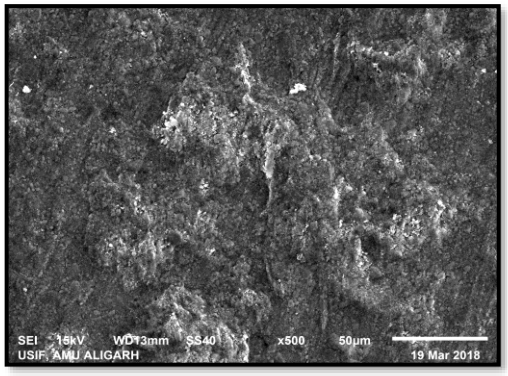

Fig. 5. SEM micrograph representing the surface morphology of the PVC/ZMP composite material.

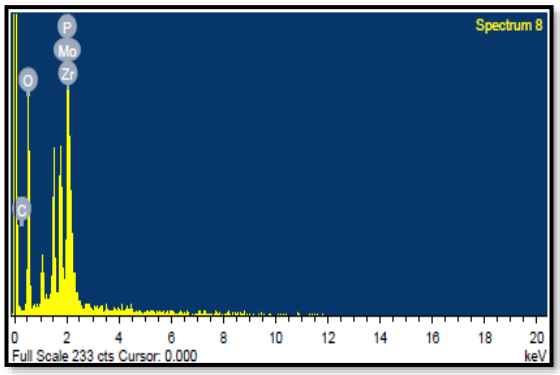

Fig. 6. EDX image of PVC/ZMP composite material.

The water content, porosity, and IEC values of the membrane were found to be 11.2, 0.17, and 0.53 meq/g of Na^+ respectively. These parameters have a great influence on the performance of the membrane as they are directly related to the transport properties of the membrane. Lower values of water content indicate that diffusion has taken place with exchangeable sites since they contain insufficient interstices. A membrane should possess optimal porosity values to give better performance, as much higher and much lower porosity values lead to the escape of water molecules or retention of exchangeable molecules, thus declining the efficiency and selectivity. It has been discovered that the composite membrane's ion exchange capacity affects membrane selectivity as well. This is because the number of exchangeable groups on the membrane matrix directly correlates with the amount of ion transport that takes place within the membrane since they serve as the ion carriers in ion exchange membranes. Additionally, it has connections to porosity and water absorption, and these factors combine to enhance membrane potential values. [31]. Chemical stability was determined by observing the results of membranes of the same composition that were soaked in different media. This process has been done by putting the synthesized membrane into different media like diluted solutions of HCl, NaOH, and NaCl for atleast 24-72 hrs. After passing time it has been observed that the membrane should be found to be chemically stable as it showed no decoloration, cracks, solubility, decomposition, or compaction when it was soaked.

The electrochemical and transport properties of an ion exchange membrane play a crucial role in understanding the performance of the membrane. These are essential parameters to foresee the execution and conduct of membranes in various applications. When a membrane is placed between two-chambered glass cells containing electrolyte solutions of different concentrations, an electric potential difference develops across the membrane due to unequal ionic flow utilizing either of the mechanisms; dissociation of functional groups or ionic adsorption from the solution. In ion exchange membranes, ion distribution is also influenced by the presence of charge on the membrane. The membrane phase contains a lower concentration of co-ions and a higher concentration of counter-ions. This difference in the concentration of ions generates an electric potential across the membrane solution interface to maintain the electroneutrality requirement between the membrane and the solution. This potential is termed the Donnan potential, which is responsible for the repulsion of co-ions and the attraction of an equal number of counter ions by the membrane, and the mechanism is termed Donnan exclusion. This potential difference causes the electric double layer across the membrane [32]. Membrane potential across the membrane was measured using 1:1 electrolytes at different concentrations and the values are plotted against the – log of concentration Fig. 7 and the results are presented in Table 2. Positive values of membrane potential signify the cation-selective nature of the membrane. The graph represents two more observations; it shows the dependence of membrane potential on electrolyte concentration as well as the nature of the electrolyte used. Both factors are explained separately. Results revealed that membrane potential values are highest in the case of NaCl followed by the order NaCl>KCl>$NaNO_3$> KNO_3, which is attributed to the small size of chloride ions in comparison to nitrate ions and similarly that of sodium ions in comparison to potassium ions. Smaller size leads to higher mobility and thus higher membrane potential values. Membrane potential shows dependence on electrolyte concentration due to two factors; changes in the double layer across the membrane occur on increasing the electrolyte concentration, which results in decreasing the co-ion exclusion and membrane potential [33]. Secondly, higher electrolyte concentrations are responsible for higher inter-ionic attractions and lower mobility and membrane potential values. The TMS model given by the scientists, Toerell, Maeyer, and Sievers, explains the theoretical prediction of membrane potential measurements, and the equation is given as follows.

$$\Delta\bar{\Psi}_m = 59.2\left(\log\frac{C_2}{C_1}\frac{\sqrt{4C_1^2+\bar{D}^2}+\bar{D}}{\sqrt{4C_2^2+\bar{D}^2}+\bar{D}}+\bar{U}\log\frac{\sqrt{4C_2^2+\bar{D}^2}+\bar{D}\bar{U}}{\sqrt{4C_1^2+\bar{D}^2}+\bar{D}\bar{U}}\right) \quad (4)$$

where $\bar{U}=(\bar{u}-\bar{v})/(\bar{u}+\bar{v})$ $\bar{u}$ and $\bar{v}$ are the cation and anion mobilities ($m^2.V^{-1}.s^{-1}$) respectively, and D is the charge density of the membrane.

From the theoretical potential values by TMS theory and experimental membrane potential values, a graph has been plotted to find out the fixed charge density. Various charge density values have been assumed at <1 for 1:1 electrolytes, and using these values, various membrane potential values were plotted along with the experimental value represented in Fig. 8. The coincidental point between the two curves represents a fixed charge density value. It follows the order of KNO_3>$NaNO_3$>KCl> NaCl, which is due to the reason that the greater ionic atmosphere is associated with the large cation size.

Table 2
Experimentally determined membrane potential values for 1:1 electrolytes at room temperature

Electrolyte Conc. C_2/C_1 (mol/l)	Observed membrane potential (mV)			
	NaCl	KCl	$NaNO_3$	KNO_3
1/0.1	14.8	13.9	13.3	12.5
0.1/0.01	20.2	19.4	18.9	18.0
0.05/0.005	26.6	26.0	25.4	24.7
0.02/0.002	35.1	34.5	33.9	33.2
0.01/0.001	39.9	39.3	38.4	37.7

Membrane transport properties are influenced mainly by the electrical charge on the membrane and the mobility of ions, and it measures the selectivity and efficiency of the membrane performance. It is defined as the total amount of current across the membrane produced due to the presence of counter-ions. It can be evaluated as follows by Eq. 5:

$$\Delta\psi_m = \frac{RT}{F}(t_+ - t_-)\ln\frac{c_2}{c_1} \tag{5}$$

where, t_+ and t_- represent the transport numbers of ions, and C_1 and C_2 are concentrations of electrolyte solutions in different chambers across the membrane. The Donnan effect can be ignored in a slightly charged membrane where diffusion potential is the main cause of membrane potential and, thus, mobility ratio may be determined by using the following equation.

$$\psi_m \approx \psi_{Diff} = \frac{RT}{F}\left[\frac{t_+}{|Z_+|} - \frac{t_-}{|Z_-|}\right]\ln\frac{c_2}{c_1} \tag{6}$$

$$U = \left[\frac{t_+}{|Z_+|} - \frac{t_-}{|Z_-|}\right] \tag{7}$$

$$\bar{\omega} = \frac{t_+}{t_-} \tag{8}$$

where, $\bar{\omega}$ signifies the mobility ratio and Z_+ and Z_- are cationic and anionic valencies respectively [34]. Both the parameter followsa similar trend as that of membrane potential and decreased with higher electrolyte concentration which is attributed to the steric hindrance in the pores of the membrane as higher concentration has resulted in lesser ionic movement and mobility and transport number due to high ionic attractions. A plot of transport numbers and mobility ratio is given in Fig. 9 and Fig. 10 respectively. So it is very clear that the higher transport number follows the high mobility ratio of ions that increases by decreasing the concentration of electrolyte solutions.

4. Conclusion

The sol-gel method of material synthesis has been used to create a PVC-based ZMP composite cation exchange membrane. Various methodologies were used to characterize the membrane's physicochemical and electrochemical properties. The membrane's structural shape was revealed by SEM analysis to be uniform and free of cracks, and EDS analysis verified the composition to be exactly as it had been created. The membrane turns out to be both chemically and thermally stable. Porosity, water content, and ion exchange values all showed positive outcomes. Values for membrane potential, transport number, and mobility ratio supported the general pattern and demonstrated reliance on electrolyte concentrations. Furthermore, fixed charge density values were calculated by TMS theory, and a close agreement between experimental and theoretical values indicates the selectivity and efficiency of the membrane for various applications.

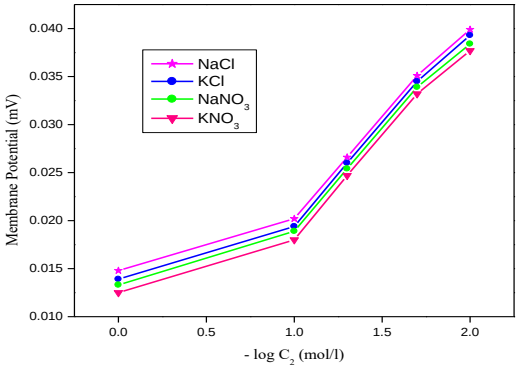

Fig. 7. Membrane potential measurement plot of various 1:1 electrolytes in contact with PVC/ZMP composite membrane.

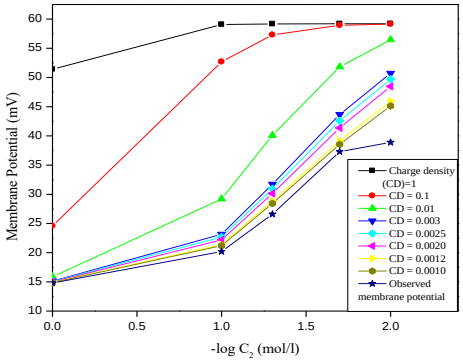

Fig. 8. Plot of membrane potential against the negative logarithm of the concentration of NaCl electrolyte solution for PVC-based TAMP composite membrane using TMS Equation for the determination of fixed charge density. Each smooth line corresponds to the theoretical values of membrane potential having $\bar{D} \leq 1$.

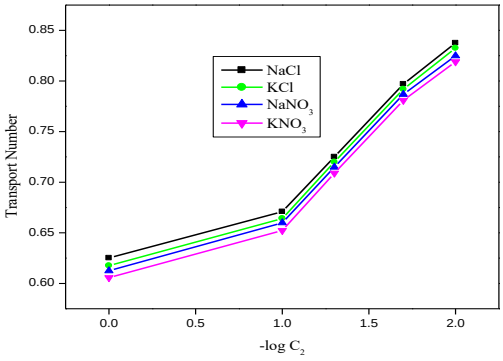

Fig. 9. Transport number plot for various electrolytes at room temperature.

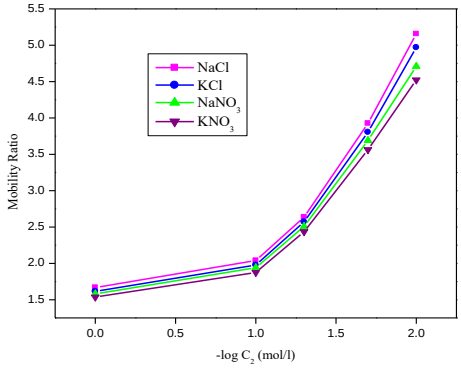

Fig. 10. Mobility ratio plot for PVC/ZMP composite membrane.

Acknowledgment

The authors would like to express their gratitude to the chairman of the Department of Applied Chemistry at AMU Aligarh for providing necessary research facilities such as FTIR, TGA/DTA, and potentiometric analysis; the Department of Physics at AMU-Aligarh for XRD analysis; and the USIF Aligarh for providing SEM facilities.

CRedit authorship contribution statement

A. Zehra: Data curation; Formal analysis.
M. Arsalan: Investigation; Methodology.
Rafiuddin: Project administration; Resources; Software; Supervision; Validation; Visualization; Writing – original draft; Writing – review & editing.

Funding

This research did not receive any specific grant from funding agencies in the public, commercial, or not-for-profit sectors**.**

Declaration of Competing Interest

The authors declare that they have no known competing financial interests or personal relationships that could have appeared to influence the work reported in this paper.

References

[1] F.W. Sefton. Fluids in the Earth's crust: Their significance in metamorphic, tectonic and chemical transport process. Vol. 1. Elsevier, 2012.
[2] G.F. Moore, J. Aiken, and S.J. Lavender. The atmospheric correction of water colour and the quantitative retrieval of suspended particulate matter in Case II waters: application to MERIS. International Journal of Remote Sensing 20.9 (1999) 1713-1733. http://dx.doi.org/10.1080/014311699212434.
[3] I. Volodymyr, Environmental microbiology for engineers. CRC Press, 2016.
[4] M. Arsalan, Rafiuddin, Binding nature of polystyrene and PVC 50:50% with CP and NP 50:50% ion exchangeable, mechanically and thermally stable membrane, J. Ind. Engg. Chem.20 (2014) 3283–3291. https://doi.org/10.1016/j.jiec.2013.11.068.
[5] A. B. Samuel, Demineralization by ion exchange: in water treatment and chemical processing of other liquids. Elsevier, 2013.
[6] B. Gianfranco, E. Dejana. Endothelial cell-to-cell junctions: molecular organization and role in vascular homeostasis. Physiol. Rev. 84.3 (2004) 869-901. https://doi.org/10.1152/physrev.00035.2003.
[7] I.A. Fauzi, and P.Y. Lai. Effects of phase inversion and rheological factors on formation of defect-free and ultrathin-skinned asymmetric polysulfone membranes for gas separation. Sep .Purif. Tchnol. 33 (2003) 127-143. http://dx.doi.org/10.1016/S1383-5866(02)00201-0.
[8] G. R., Gregory et al. Preparation and characterization of membranes formed by nonsolvent induced phase separation: a review. Ind. Eng. Chem. Res. 50 (2011) 3798-3817. http://dx.doi.org/10.1021/ie101928r.
[9] L. Cuijing, et al. Organic solvent reverse osmosis membranes for organic liquid mixture separation: A review. J. Membr. Sci. 620 (2021) 118882. https://doi.org/10.1016/j.memsci.2020.118882.
[10] M.M.A. Khan, Rafiuddin, Inamuddin, Electrochemical characterization and transport properties of polyvinyl chloride-based carboxy methyl cellulose Ce(IV) molybdophosphate composite cation exchange membrane, J. Ind. Eng. Chem. 18(2012)1391–1397. https://doi.org/10.22079/jmsr.2017.24343..
[11] P.O. Albo, H. Takaba, I. Kumakiri, An Overview of Molecular Simulations Studies in Mixed Matrix Membranes for Gas Separation Processes, J. Membr. Sci. Res. http://www.msrjournal.com/article_253969.html.
[12] N. D. Long, A.I. Schäfer, M. Elimelech. Role of electrostatic interactions in the retention of pharmaceutically active contaminants by a loose nanofiltration membrane. J. Membr. Sci. 286.1-2 (2006) 52-59. http://dx.doi.org/10.1016/j.memsci.2006.09.011.
[13] R. Kumar. Vinoth, et al. Performance assessment of an analcime-C zeolite–ceramic composite membrane by removal of Cr (VI) from aqueous solution. RSC Adv. 5 (2015) 6246-6254. https://doi.org/10.1039/C4RA14527E.
[14] M.M.A. Khan, Rafiuddin, Inamuddin, Electrochemical characterization and transport properties of polyvinyl chloride-based carboxy methyl cellulose Ce(IV) molybdophosphate composite cation exchange membrane, J. Ind. Eng. Chem. 18 (2012) 1391–1397. https://doi.org/10.22079/jmsr.2017.24343.
[15] K. Ghasemzadeh, A.A. Meybodi, A. Iulianelli, A. Basile, Theoretical Performance Evaluation of Inorganic (Non-Pd-Based) Membranes for Hydrogen Separation, J. Membr. Sci. Res. 4 (2018) 198-203. https://doi.org/10.22079/jmsr.2018.74280.1160.
[16] Li, Jian, et al. Mussel-inspired monovalent selective cation exchange membranes containing hydrophilic MIL53 (al) framework for enhanced ion flux. Ind. Eng. Chem. Res. 57.18 (2018) 6275-6283. http://dx.doi.org/10.1021/acs.iecr.8b00695.
[17] Zhao, Yan, et al. Nanofiber based organic solvent anion exchange membranes for selective separation of monovalent anions. ACS Appl. Mater.Interf.12 (2020) 7539-7547. https://doi.org/10.1021/acsami.9b19962.
[18] M. Arsalan, Rafiuddin, Fabrication, characterization, transportation of ions and antibacterial potential of polystyrene-based Cu3 (PO4)2/Ni3 (PO4)2 composite membrane, J. Ind. Engg. Chem.20 (2014) 3568–3577. http://dx.doi.org/10.1016/j.jiec.2013.12.050.
[19] Z.A. Siddiqi, M. Khalid, S. Kumar, M. Shahid, S. Noor, Antimicrobial and SOD activities of novel transition metal complexes of pyridine-2, 6-dicarboxylic acid containing 4-picoline as auxiliary ligand, E. J. Med. Chem. 45 (2010) 264-9. https://doi.org/10.1016/j.ejmech.2009.10.005.
[20] A. Cahil, M. Najdoski, V. Stefov, Infrared and Raman spectra of magnesium ammonium phosphate hexahydrate (struvite) and its isomorphous analogues. IV. FTIR spectra of protiated and partially deuterated nickel ammonium phosphate hexahydrate and nickel potassium phosphate hexahydrate. J. Mol. Str.834 (2006) 408–413. https://pubmed.ncbi.nlm.nih.gov/24062107/.
[21] M.N. Beg, M.AZ. Matin, Studies with nickel phosphate membranes: evaluation of charge density and test of recently developed theory of membrane potential, J. Membr. Sci.196 (2002) 95–102. http://dx.doi.org/10.1016/S0376-7388(01)00582-8.
[22] D.E. Vlotman, J.C. Ngila, T. Ndlovu, S.P. Malinga, Hyperbranched Polymer Integrated Membrane for the Removal of Arsenic(III) in Water, J. Membr. Sci. Res.4 (2018) 53-62. http://dx.doi.org/10.22079/JMSR.2017.67560.1148.
[23] T. Arfin, Rafiuddin, An electrochemical and theoretical comparison of ionic transport through a polystyrene-based cobalt arsenate membrane, Electro. Acta56 (2011) 7476–7483. http://dx.doi.org/10.1016/j.desal.2011.02.014.
[24] G. Enver, et al. Performance-determining membrane properties in reverse electrodialysis. J. Membr. Sci. 446 (2013) 266-276. http://dx.doi.org/10.1016/j.memsci.2013.06.045.
[25] A.A. Khan, U. Habiba, S. Shaheen, M. Khalid, Ion-exchange and humidity sensing properties of poly-o-anisidine Sn(IV) arsenophosphate nano composite cation-exchanger, Journal of Environmental Chemical Engineering 1 (2013) 310–319, J. Envir. Chem. Eng. 1 (2013) 310–319. http://dx.doi.org/10.1016/j.jece.2013.05.010.
[26] H. Matsumoto, Y.C. Chen, R. Yamamoto, Y. Konosu, M. Minagawa, A. Tanioka, Membrane potentials across nanofiltration membranes: effect of nanoscaled cavity structure, J. Mol. Str.739 (2005) 99–104. https://ui.adsabs.harvard.edu/link_gateway/2005JMoSt.739...99M/doi:10.1016/j.molstruc.2004.05.038.
[27] L. Chaabane, G. Bulvestre, C. Innocent, G. Pourcelly, B. Auclair, Physicochemical characterization of ion-exchange membranes in water–methanol mixtures, Euro. Poly. J.42 (2006) 1403–1416. http://dx.doi.org/10.1016/j.eurpolymj.2005.12.019.
[28] M. L. Hir, Y. Wyart, G. Georges, L. Siozade, P. Moulin, Nanoparticles Retention Potential of Multichannel Hollow Fiber Drinking Water Production Membrane, J. Membr. Sci. Res.4 (2018) 74-84. https://doi.org/10.22079/jmsr.2017.69079.1150.
[29] Tanvir Arfin, Rafiuddin, Transport studies of nickel arsenate membrane, Journal of Electroanalytical Chemistry636 (2009) 113–122. https://doi.org/10.1016/j.jelechem.2009.09.019.
[30] A.A. Moya, Harmonic analysis in ideal ion-exchange membrane systems Electro.Acta.90 (2013) 1– 11.
[31] M. Géraldine, M. Wessling, K. Nijmeijer. Anion exchange membranes for alkaline fuel cells: A review. J. Membr. Sci. 377 (2011) 1-35. http://dx.doi.org/10.1016/j.memsci.2011.04.043.

[32] U. Ishrat, Rafiuddin, Synthesis characterization and electrical properties of Titanium molybdate composite membrane. Desalination 286 (2012) 8–15. http://dx.doi.org/10.1016/j.desal.2011.11.059.

[33] M. Arsalan, Rafiuddina, Synthesis, structural characterization, electrochemical, and electrical study of polystyrene-based manganous tungstate composite cation exchange membrane, Desalin. Water Treat. 52 (2014) 7531-7542. doi: 10.1080/19443994.2013.831793. http://dx.doi.org/10.1080/19443994.2013.831793.

[34] M.M.A Khan, Rafiuddin. Synthesis, characterization and electrochemical study of calcium phosphate ion exchange membrane, Desalination272 (2011) 306–312. http://dx.doi.org/10.1016/j.desal.2011.01.041.